

Coupling of the GOTM turbulence module to some three-dimensional ocean models

MANUEL RUIZ VILLARREAL
(manuel.ruiz@co.ieo.es), KARSTEN
BOLDING, HANS BURCHARD, and
ENCHO DEMIROV

26.1 Introduction

In this chapter, the coupling of the GOTM to various ocean models will be described. These models have been designed for different oceanic regimes; namely the open ocean (the Modular Ocean Model [MOM]; see Pacanowski and Griffies [1999]) and estuarine and coastal flows (the Modelo Hidrodinámico [MOHID]; see Martins *et al.* [1998], Burchard and Bolding [2002], with the General Estuarine Transport Model [GETM]) and can be taken as representatives of the variety of ocean models used by the modelling community. The MOM is a rigid-lid model that uses a classical geopotential coordinate, whereas the MOHID and GETM are free-surface models that use a generic vertical-coordinate approach. This allows the use of sigma or Cartesian approaches, or a combination of them, in the vertical. The physical regimes that will be modeled range from a mesoscale application; the MOM applied to the Mediterranean Sea, a wind-driven shelf; through the Portuguese–Galician shelf on the Iberian margin, to a shallow tidal embayment with intertidal flats the Sylt–Rømø Bight in the Wadden Sea. The different dynamic regimes are described with the same turbulence model, making use of the improved two-equation closures in the GOTM, which are described in Burchard and Bolding (2001). In these applications, the use of a second-order turbulence closure will be shown to improve the predictions of the model.

26.2 Interfacing between hydrodynamic and GOTM turbulence modules

The turbulence module in the GOTM constitutes an independent module, which makes it possible to use it as the turbulence module of any three-dimensional model. In these applications, no advection of turbulence has been considered. Therefore, at every horizontal point of the model, a one-dimensional vertical system is solved. Vertical diffusion is solved implicitly in all of the models. Two of the models presented discretize the equations in an Arakawa C grid (the GETM and MOHID); the other (the MOM) does it in an Arakawa B grid. This has the consequence that the

locations of turbulence magnitudes in the horizontal and the consequent interpolations differ. A vertical staggering of the grid is considered in all of them, with turbulence magnitudes located at the interfaces between mean-flow points.

26.3 The MOM applied to the Mediterranean Sea

The MOM was developed in the Geophysical Fluid Dynamics Laboratory (GFDL), Princeton, USA. It was originally designed by Bryan (1969) as a three-dimensional primitive-equation, rigid-lid, and hydrostatic z -coordinate model. On the basis of this work, Mike Cox constructed in 1968 a global ocean-circulation model. Modified versions of this model were developed by Semtner (1974) and Cox (1984). Pacanowski *et al.* (1991) rewrote the Cox (1984) model introducing a modular structure. This was the first MOM (MOM.1). In the next version of the model, MOM.2, the architecture was significantly modified, which increased the flexibility in parallelization of the code and optimized it for use on multiple processors. The latest freely available version of the model, MOM.3 (Pacanowski and Griffies, 1999), is written in FORTRAN 90 and has new options for the parameterization of the subgrid physical processes and new features of the numerical scheme. The new options in MOM.3 together with the modular structure of the model increase the flexibility of the model for use in ocean-circulation studies.

Since the beginning of the 1990s the MOM has been used in a number of model studies of the Mediterranean Sea circulation. Malanotte-Rizzoli and Bergamasco (1991) applied MOM.1 in simulation of the eastern Mediterranean Sea. The same model was employed by Bergamasco *et al.* (1993) together with an adjoint method in a study of the steady-state circulation in the basin. Roussenov *et al.* (1995) implemented MOM.1 for the whole Mediterranean. The original version of this model, which hereafter will be referred to as the Mediterranean MOM, had 0.25° resolution and 19 vertical levels. The transport through the Straits of Gibraltar was parameterized by extension of the numerical

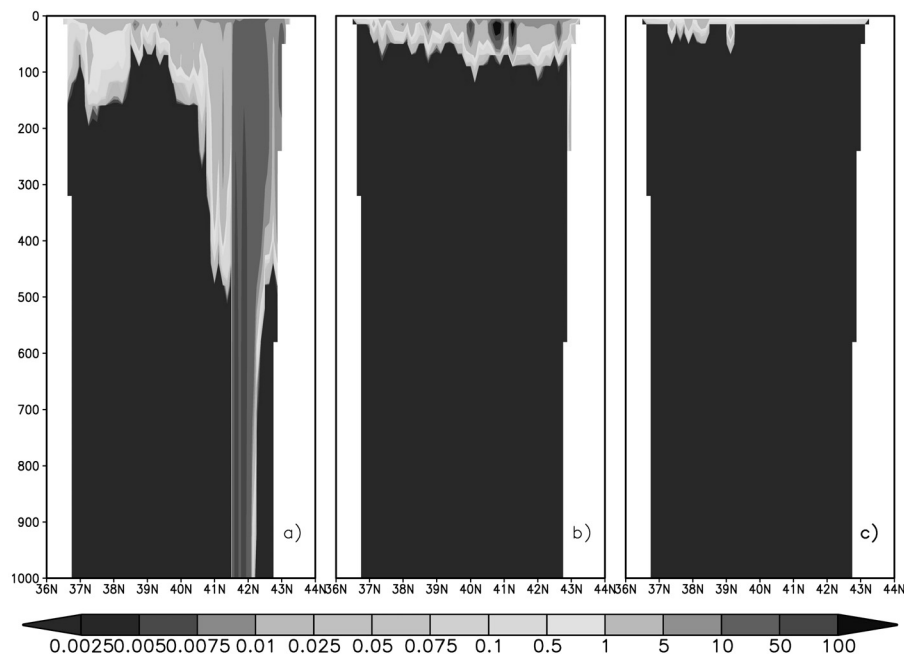


Fig. 26.1. Meridional vertical cross sections of turbulence kinetic energy at 5°E: (a) February 14, 2000; (b) March 14, 2000; and (c) August 14, 2000. In color on the CD.

grid westward and inclusion in the model area of a part of the north Atlantic Ocean. Pinardi and Navarra (1993) and Roussenov *et al.* (1995) applied the Mediterranean MOM in a study of the seasonal variability of the sea. Pinardi *et al.* (1997), Korres *et al.* (2000), and Castellari *et al.* (2000) used the Mediterranean MOM with 31 vertical levels in simulations of the interannual variability of the Mediterranean. Wu and Haines (1996) and Wu *et al.* (2000) applied the model with resolution 0.25° and 0.125° degree and 41 vertical levels in studies of physical processes of formation of the deep and intermediate water masses. At present the Mediterranean MOM is a part of the Mediterranean Forecasting System (MFS; see Pinardi *et al.* [2001]), which produces weekly basin-scale forecasts of hydrodynamic fields.

26.3.1 Simulation of the circulation in the Mediterranean Sea

The Mediterranean Sea is a semi-enclosed basin consisting of two parts – eastern (EMED) and western (WMED), which communicate through the relatively narrow Sicily Strait. The circulation and water-mass structure of the sea is influenced by a relatively large range of physical processes and their interaction; see Robinson and Golnaraghi (1994). Deep and intermediate-depth winter convection and overturning thermohaline circulation play important roles for the overall variability of the basin. At the same time the dynamics of the regional seas (e.g. Adriatic

and Aegean) and the transport through the relatively shallow and narrow straits are important factors for the variability of the circulation in the deep part of the Mediterranean.

The thermohaline circulation in the Mediterranean consists of one zonal vertical cell in the whole Mediterranean and two meridional cells, one in the EMED and one in the WMED. The zonal cell is composed by a flow of surface modified Atlantic waters toward the easternmost part of the Mediterranean and westward flow of salty Levantine intermediate waters. The two meridional thermohaline cells are related to the processes of deep convection and formation of deep waters in the EMED and the WMED, respectively.

The western Mediterranean deep water is produced by the deep convection in the Gulf of Lions (Leaman and Schott, 1991). The deep water of the EMED forms in the semi-enclosed Adriatic or Aegean Seas and then fills the deep part of the basin (Roether and Schlitzer, 1991; Roether *et al.*, 1996).

26.3.2 Implementation of the GOTM in the Mediterranean MOM

Here we present some preliminary results from simulation of the region of Gulf of Lions produced by the Mediterranean MOM with the GOTM. The period of the simulation is from January to August 2000. Both data and MFS analysis (Demirov and Pinardi, 2002) show that deep convection events occurred during the first two months of

2000. The aim of our preliminary study is to evaluate the impact of the turbulence scheme on the model solution during and after the deep convection period.

The Mediterranean MOM has horizontal resolution of $0.125^\circ \times 0.125^\circ$ and 31 vertical levels. The surface heat and momentum fluxes are computed in an interactive way by using the sea-surface temperature from the model and 6 h of atmospheric parameters from European Center for Medium-Range Weather Forecasts (ECMWF) analysis. The model is initialized with MFS analysis for January 1, 2000 and is run to August 2000 with forcing computed from 6 h of ECMWF analysis. This is the version of the Mediterranean MOM which is at present being used in the MFS and a more detailed description can be found in Demirov and Pinardi (2002).

The vertical mixing in the Mediterranean MOM of the MFS is parameterized with constant coefficients of turbulent diffusion and viscosity. A convective adjustment (Cox, 1984) procedure is applied in areas of vertical static instability. In addition MFS analysis is computed with assimilation of observations from the MFS observing system. The assimilated data set includes expendable-bathythermograph temperature profiles, satellite sea-surface temperatures, and sea-level-anomaly data.

In our simulations the original vertical mixing scheme of the MFS version of the model with constant mixing coefficients is replaced by the GOTM implementation (Burchard and Bolding, 2001) of the $k-\varepsilon$ turbulence model with stability functions of Canuto *et al.* (2001). The GOTM is coupled with the MOM through an interface subroutine (not by direct implementation in the MOM). The reason for this choice is that several versions of the GOTM have been released during recent years. The input to the interface is the position of the model point and the outputs (used by the MOM) are the turbulent diffusivity and viscosity. The MOM has a B-staggered numerical grid. The turbulence characteristics are calculated by GOTM code on the tracer points. The interface interpolates linearly the velocity components at the tracer model points before the shear-stress computations and then passes them, together with the buoyancy frequency and wind stress, to the GOTM. The turbulent viscosities, which are computed from the GOTM, are interpolated by the interface at the velocity grid points and then are provided, together with turbulent diffusivities, to the MOM code.

As mentioned above, the MFS model is based on the MOM.1 version of the GFDL ocean general-circulation model (OGCM). Even though this is not the latest version of the MOM code, we use it in the tests of the GOTM–MOM implementation since it provides us with an opportunity to use the experience and data from the MFS simulations in the evaluation of the impact of the GOTM mixing scheme. At the same time the GOTM–MOM implementation is

relatively simple and easily applicable in more recent versions of the MOM.

Here we discuss the three-dimensional OGCM simulations with the Mediterranean MOM and GOTM for three periods of time – during a deep convection event in the middle of February, one month later (i.e. in the middle of March), and at the end of the simulations.

26.3.3 Simulation of the western Mediterranean Sea with the MOM

The strong surface cooling during the winter of 2000 forced deep convection events in the Gulf of Lions at the end of January and in early February. Strong vertical mixing and vertical homogenization of the water column were observed in MFS data and analysis in the central part of the cyclonic gyre, which is present quasi-permanently in the region.

The turbulence kinetic energy (TKE) and vertical diffusion computed from the $k-\varepsilon$ turbulence model are shown in Fig. 26.1 and 26.2. The TKE distribution reveals a strong maximum in February in the region 41.5°N – 42°N at longitude 5°E , i.e. in the central part of the cyclonic gyre (Fig. 26.1(a)). Correspondingly the vertical diffusion (Fig. 26.2(a)) in the whole column in this area increases to about $1\text{ m}^2\text{ s}^{-1}$, which produces fast homogenization of the water column. In March the TKE (Fig. 26.1(b)) and vertical turbulent diffusion (Fig. 26.2(b)) remain high in the surface 100-m layer, whereas in August (Figs. 26.1(c) and 26.2(c)) the vertical mixing is relatively strong only in a shallow surface layer. The vertical turbulent mixing at depths 150–250 m in the well-stratified area of Algerian current are relatively weak throughout the whole period (Figs. 26.1 and 26.2). In the Gulf of Lions the vertical diffusion at intermediate and deep levels reveals strong seasonal variations. During the winter the vertical diffusion there is relatively high due to the processes of vertical convection, whereas in spring and summer it decreases monotonically.

The horizontal velocity and temperature distribution at 100 m (Fig. 26.3) in the southern part of the Algerian–Provençal Basin reveals a strong mesoscale variability in the area of Algerian current. During the whole year energetic eddies of size of 100–150 km are observed in the model velocity and temperature fields. In the northern part of the WMED, the circulation is cyclonic throughout the whole period of simulation. The circulation strongly intensifies during February, with relatively high velocities in the area of the deep convection. The cold waters formed here during the winter remain “captured” by the cyclonic gyre throughout the whole period of simulation. In February and March the exchange between waters inside and outside the cyclonic gyre is mainly due to the outflow of cold waters along the coasts of Mallorca and inflow of warm waters originating west Sardinia. In summer the outflow from the Gulf of Lions is not present (Fig. 26.3(c)).

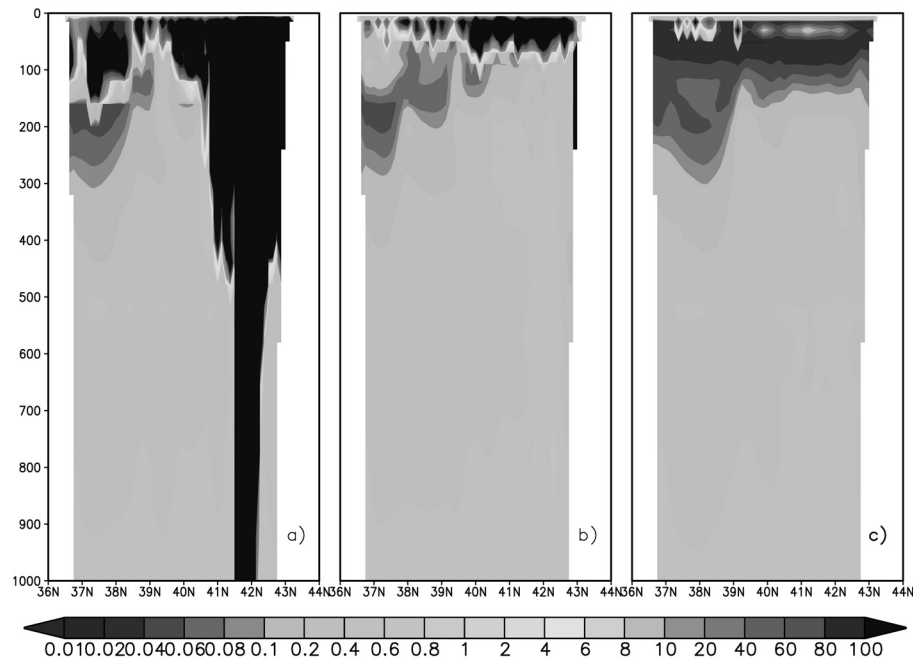


Fig. 26.2. Meridional vertical cross sections of eddy diffusivity at 5°E: (a) February 14, 2000; (b) March 14, 2000; and (c) August 14, 2000. In color on the CD.

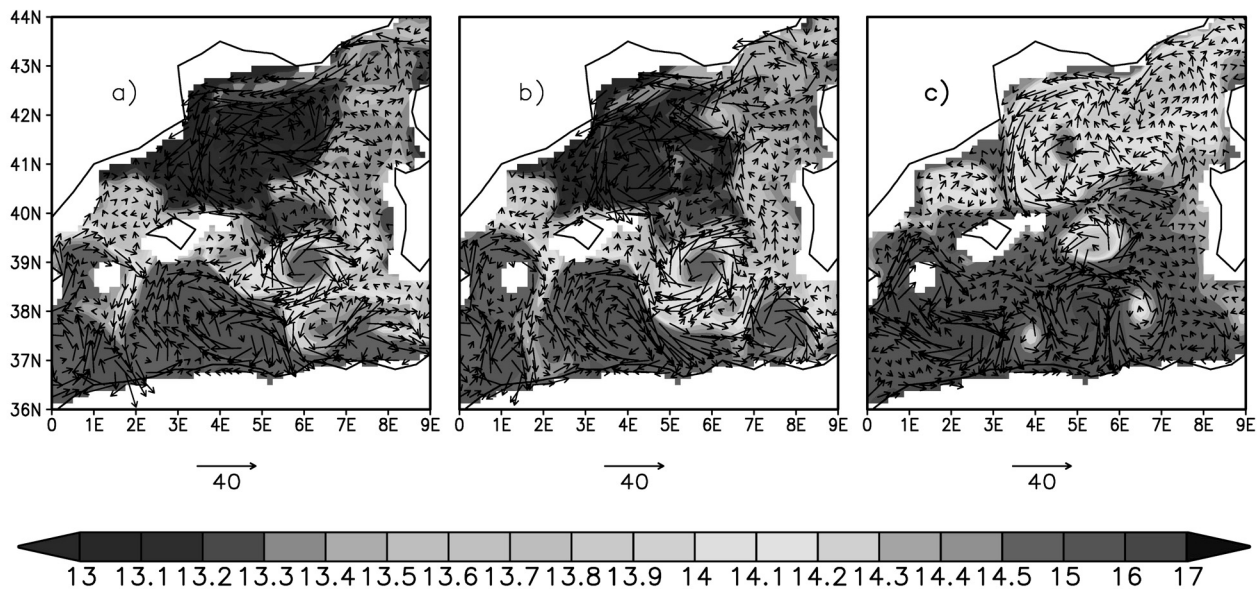


Fig. 26.3. Horizontal temperature and velocity distributions at 100 m depth on (a) February 14, 2000; (b) March 14, 2000; and (c) August 14, 2000. In color on the CD.

The area of cold deep waters at depth 1000 m formed during the deep convection in February 2000 is located in the central part of the cyclonic gyre (Fig. 26.4(a)). The size of the area corresponds well to the observations (Leaman and Schott, 1991), which suggest that the deep convection has a horizontal scale of about 50–100 km. In March the area

of cold waters extends zonally to about 42°N. Following the cyclonic direction of the flow in the gyre, the cold waters propagate to the west and along the coast (Fig. 26.4(b)). During the spring and summer, the horizontal mixing decreases the contrast of the temperature in the area of winter deep convection. In August the cold waters are hardly seen

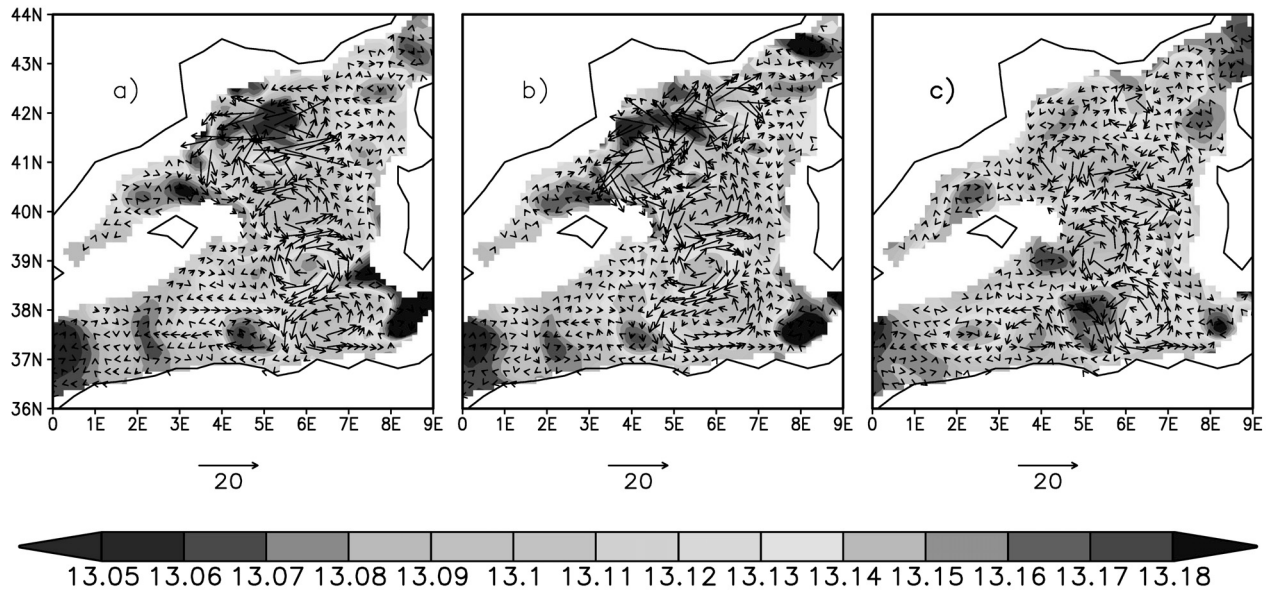


Fig. 26.4. Horizontal temperature and velocity distributions at 1000 m depth on (a) February 14, 2000; (b) March 14, 2000; and (c) August 14, 2000. In color on the CD.

in the distribution of the temperature field (Fig. 26.4(c)). At the same time the circulation in the cyclonic gyre of the Gulf of Lions weakens at all levels during the summer season.

The model results show that the GOTM–MOM simulations represent well the major features of the winter convection in the Gulf of Lions. The convection appears in the central part of the cyclonic gyre of the Gulf of Lions. The variability of the cold waters formed during the winter months is related to the dynamic features of the cyclonic circulation in the region. The model solution suggests that the deep water formed during winter remains relatively stable throughout the whole period of simulations with slowly evolving temperature.

26.4 The MOHID applied to the Iberian west coast

26.4.1 A general introduction to the MOHID

The MOHID is a three-dimensional baroclinic model that was originally developed by the MARETEC group (Instituto Superior Tecnico, Universidade Tecnica de Lisboa, Lisbon, Portugal). Several different estuaries and coastal areas have been modeled with the MOHID in the framework of research and consulting projects. The model has been applied to most of the tidal estuaries on the Iberian Atlantic coast (Martins *et al.*, 2001; Taboada *et al.*, 1998; Villarreal *et al.*, 2001) and also to some other European estuaries – the Western Scheldt (the Netherlands) and the Gironde (France) (Cancino and Neves, 1999). The MOHID has also been applied to the Iberian shelf and shelf

break during the Ocean Margin Exchange project¹ (Coelho *et al.*, 2002). The model solves the primitive equations using a finite-volume method. In this approach, the governing equations are expressed as conservation laws in a control volume, where all terms in the primitive equations appear as fluxes or sink–source terms in this conservation law. No coordinate transformation is applied to the equations and geometrical information is carried in the areas and volumes needed to calculate the fluxes. With this method, a separation of geometry and hydrodynamics is accomplished. Depending on the specified coordinate, the shape of the control volume will vary during the course of the calculus and therefore geometry is updated at every time step. At this moment in the development of the model, the control volumes are allowed to vary only in the vertical, and this approach is equivalent to having a generic vertical coordinate; i.e. Cartesian, sigma, or isopycnal layers, or even a combination of them, can be chosen as vertical coordinates. The temporal discretization is carried out with an ADI Alternate Direction Implicit algorithm. This algorithm computes alternately one component of velocity implicitly while the other is calculated explicitly. This method has the advantage accruing from the stability of implicit methods without their drawbacks of computational expensiveness and associated phase errors. Additionally, the MOHID is equipped with a stable drying–flooding algorithm, which extends its applicability to areas with intertidal flats.

¹ <http://www.pol.ac.uk/bodc/omex/omex.html>.

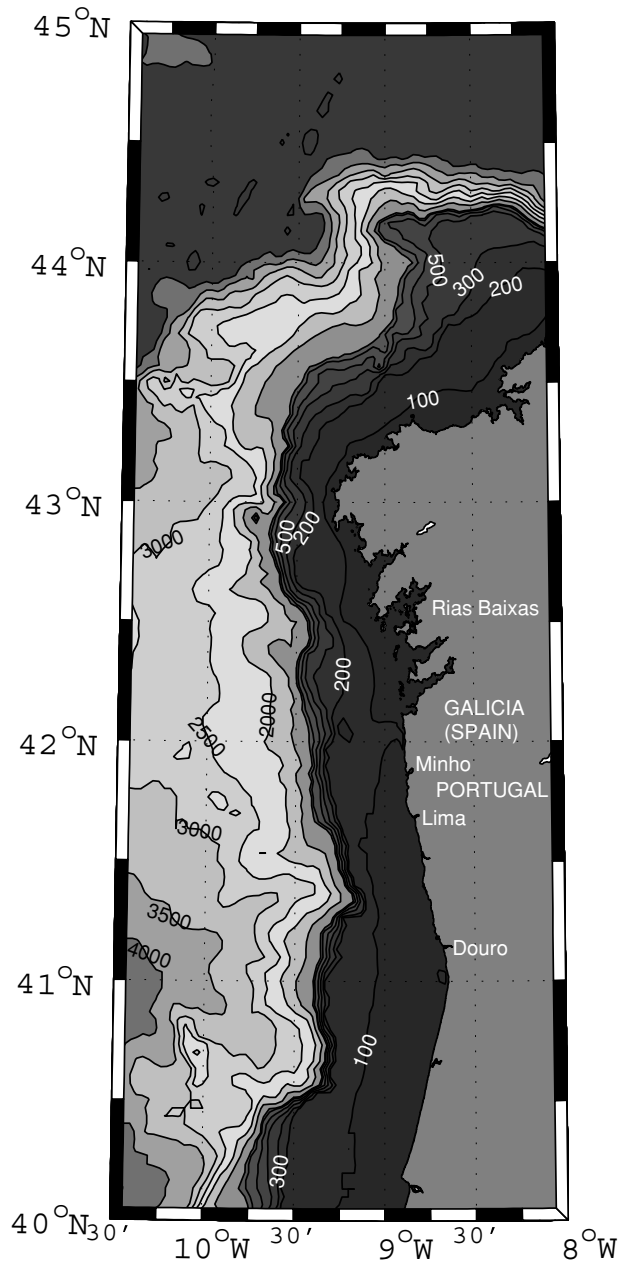


Fig. 26.5. Bathymetry of the simulated part of the Iberian shelf used in the numerical model. In color on the CD.

26.4.2 Coupling of the GOTM with the MOHID

In the MOHID, where magnitudes are discretized in an Arakawa-C grid scheme, turbulence quantities are horizontally located at tracer points. Vertically, the staggering of the grid is like that in the GOTM, where mean-flow quantities are located at the center of the control volume and turbulence magnitudes at the faces. However, care has to be taken with the numbering of layers, which differs between the MOHID and the GOTM. Consequently, shear

and buoyancy terms in the turbulence equations have to be computed at the center of the vertical faces of the control volume. Shear stress can be alternatively computed by horizontally averaging velocities at tracer points and then computing the vertical velocity gradient or by computing the shear-production term at velocity points and then interpolating this value to tracer points. Buoyancy production is easily computed at tracer points, where N^2 is defined, without any horizontal averaging.

From a computational-architecture point of view, the latest version of the model was written following an object-oriented architecture and the model is fully modular. Owing to this advanced conception and the modular character of the GOTM, it has easily been adapted as the module for predicting turbulent exchange coefficients in the MOHID. Only minor modifications have been made to the original GOTM subroutines and an object interface has been developed for transferring information between the three-dimensional model and the one-dimensional column MOHID.

26.4.3 The wind-driven Portuguese–Galician shelf under strong river run-off

The Portuguese–Galician shelf (Fig. 26.5) is a very productive ecosystem, where spring and summer upwellings induce a renewing of nutrients and thus enhance productivity. There have been some studies of hydrodynamics in the area (for a review, see Coelho *et al.* [2002]), that have revealed the differences between summer and winter circulation, which are mainly caused by the change in mesoscale winds. We will show here an application of the MOHID to the shelf under winter conditions. We will try to investigate conditions similar to those occurring in April 2001, when rainfall and wind velocities were high and run-off of rivers discharging in the area reached flood conditions. In this situation, although not much measured information is available, it is expected that a thin layer of freshwater at the surface overlies oceanic waters. We will investigate coastal circulation during the passage of a storm under such stratified conditions.

The river run-off in the rivers in the area (Douro, Lima, Minho, and the Galician rivers) is set to flood values. The wind stress is taken from numerical results of the forecast model run at the Galician Meteorological Observation and Forecast Unit at the Universidad de Santiago de Compostela (Spain). Ten days of wind stresses every 10 min at a point on the shelf are available and will be used to force the model (see Fig. 26.6). Spatial variations of wind stress in the modeled domain are neglected for this process study.

In Fig. 26.7, velocity and salinity fields for the peak of the storm on April 6, 2001 are shown. At the surface, a strong flow northward is apparent on the inner shelf,

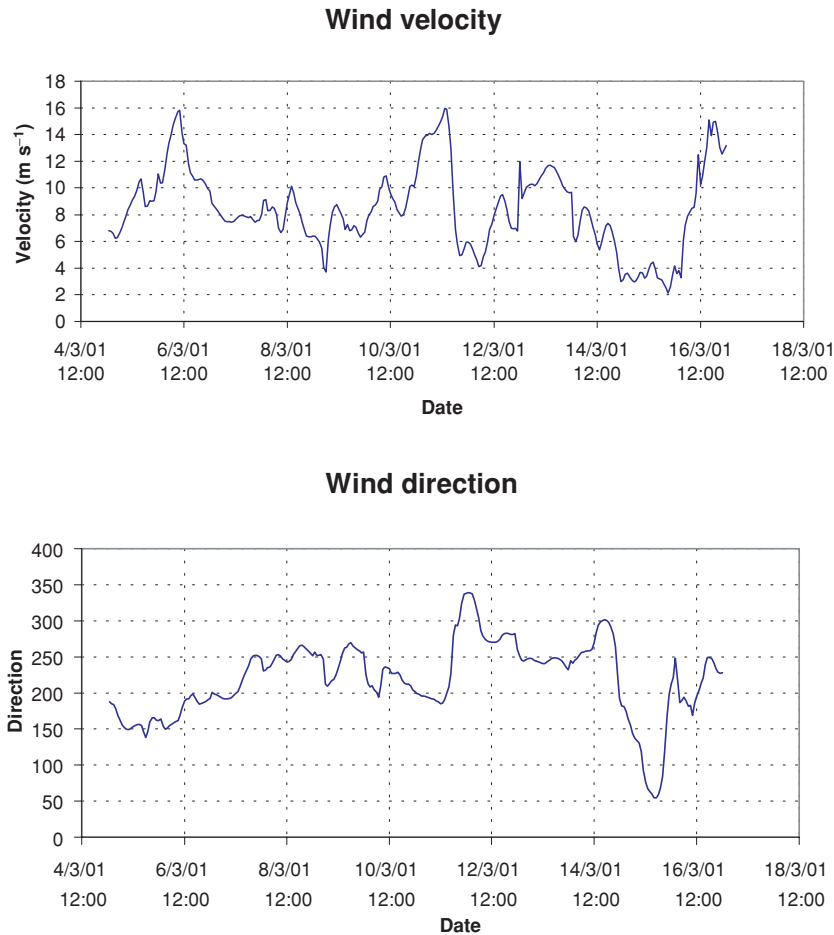


Fig. 26.6. Wind modulus and direction in a point of the shelf offshore of Oporto predicted by a numerical model.

which weakens as it advances northward. Maximum velocities reach 1 m s^{-1} near the mouth of the Douro, which had not hitherto been observed. Usual non-tidal velocities under winter conditions in the area are of the order of tenths of a centimeter per second (for a review, see Coelho *et al.* [2002]). In the salinity field, the jets corresponding to the various rivers are evident, especially that of the Douro, which reached a run-off of $10\,000 \text{ m}^3 \text{ s}^{-1}$. However, the plume of the rivers is confined to the inner shelf (about 50 km from the coast). In Fig. 26.7 (lower panel), salinities and velocities at 100 m depth are represented. It can be seen how a strong stratification appears, with freshwater plumes confined to the first few meters and ocean waters below. Velocities have the usual order of magnitude under winter conditions and are directed southward, in contrast to surface northward velocities.

The adequate description of vertical mixing (the $k-\varepsilon$ model, extended by the algebraic second-moment closure of Canuto *et al.* [2001]) allows us to model the conditions of strong run-off combined with strong winds. A narrow

layer of freshwater is confined to the first few meters and can be very effectively dragged by wind, which results in strong velocities, much faster than the usual velocities in the zone.

26.5 The GETM applied to the Wadden Sea

26.5.1 A general introduction to the GETM

The GETM was originally designed for simulating tidal flow in Wadden Sea regions that are characterized by flow strongly influenced by bottom topography and extensive areas that successively dry out and flood again (intertidal flats); see Burchard (1998) and Stanev *et al.* (2003). A baroclinic version for estuaries, coastal seas, and shelf seas is now also available (Burchard Bolding 2002; Burchard *et al.*, 2003a) For the calculation of the free-surface elevation and the vertically integrated transports a much smaller time step is chosen than for the vertical distribution of quantities and for the turbulence model. This so-called mode splitting guarantees also a stable calculation of the vertically integrated flow, including movable lateral boundaries as an

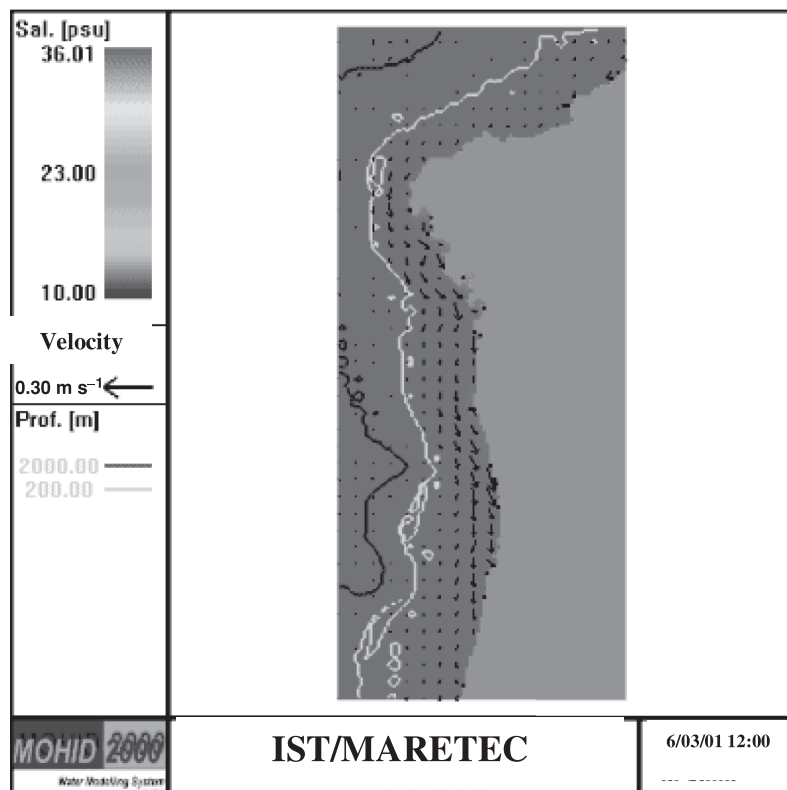
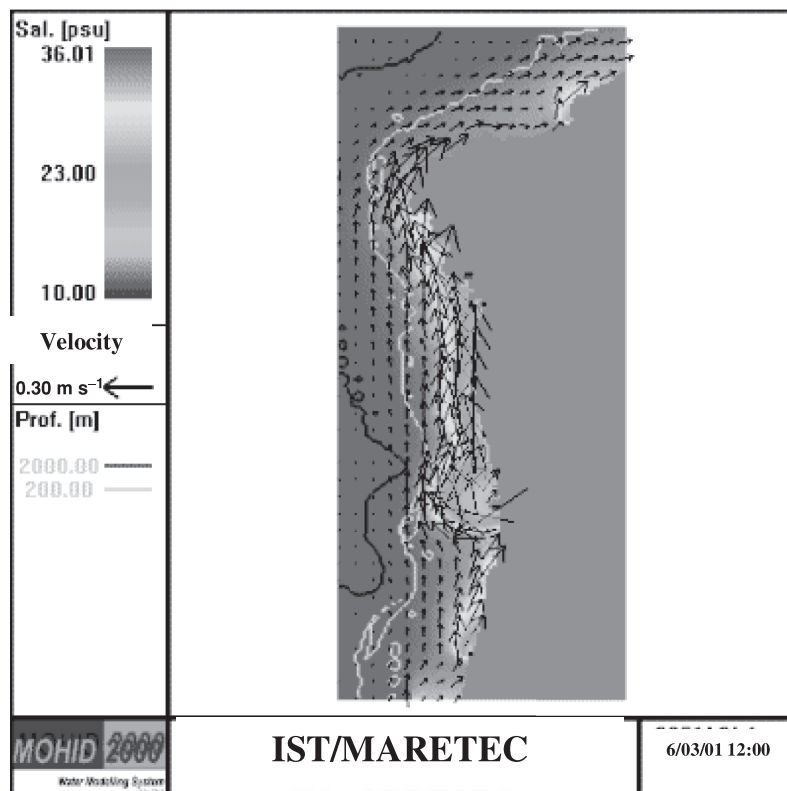


Fig. 26.7. Currents and salinity fields (a) at the surface and (b) at a depth of 100 m during the peak of the storm on April 6, 2001. In color on the CD.

Bathymetry of Sylt-Rømø Bight

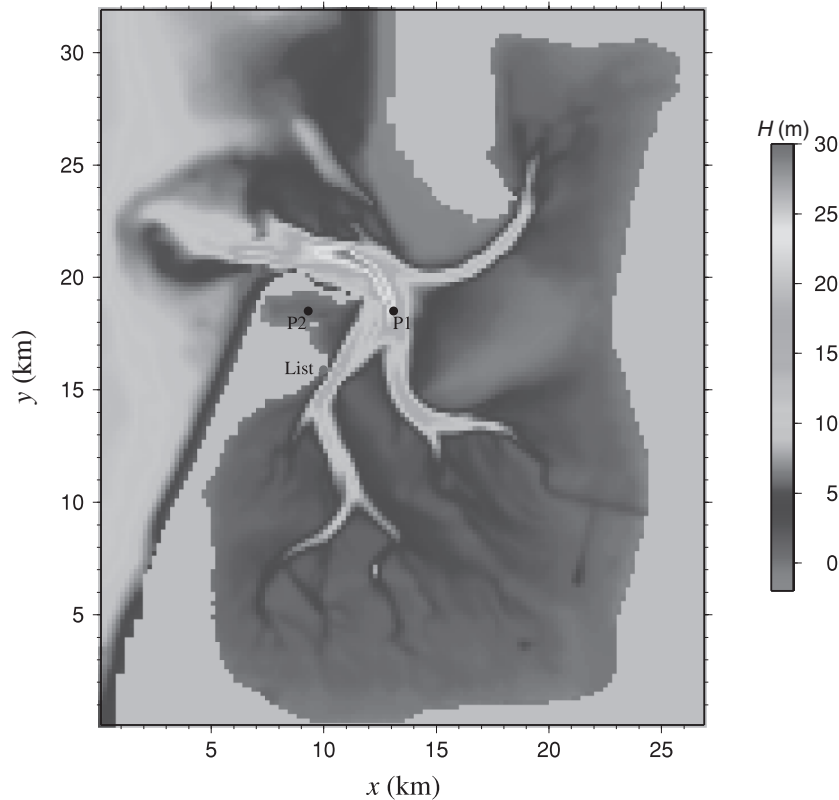


Fig. 26.8. Bathymetry of the Sylt-Rømø Bight used in the numerical model. The purple color indicates intertidal flats. The points P1 and P2 show the locations where the temporal evolution of the water column is shown; see Figs. 26.10 and 26.11. In color on the CD.

economic use of computer time. The vertical coordinate on which the model is based is a so-called general vertical coordinate (Deleersnijder and Ruddick, 1992) where by a fixed number of vertical layers is more or less arbitrarily redistributed over the water body during each time step. In the horizontal plane an Arakawa and Lamb (1977) C grid, either in Cartesian or in curvilinear coordinates, can be used, the latter including also spherical coordinates. Additionally, the GETM is now equipped with an advection-diffusion module for tracers. Various high-resolution, monotonicity-preserving advection schemes are implemented for momentum and tracers, all based on a directional-split method allowing one-dimensional schemes to be applied for this three-dimensional model. The use of these schemes can easily be extended to the advective transport of turbulence quantities which has so far been neglected.

In early versions, a simple two-equation $k-\varepsilon$ model had been integrated directly into the model; see Burchard (1997, 1998). Now, the GOTM turbulence module is linked to the GETM; see Section 26.5.2. In the Wadden Sea application presented here, the two-equation $k-\varepsilon$ model, extended by the algebraic second-moment closure of Canuto

et al. (2001), will be compared with the performance of a simple parabolic eddy-viscosity profile depending only on the bed stress.

26.5.2 Coupling of the GOTM with the GETM

In the GETM, the turbulence quantities such as TKE, dissipation rate, and eddy viscosity and diffusivity are located on the tracer points, such that the GOTM is located at these tracer points as well. As in the GOTM, so also in the GETM, the vertical staggering of the grid is carried out in such a way that the turbulence quantities are located on the interfaces between the tracer reference boxes. Technically, one subroutine is responsible for extracting one-dimensional profiles of shear production and buoyancy production from the three-dimensional fields provided by the hydrodynamic model. Then, the GOTM turbulence module is called with these one-dimensional forcing profiles successively for all horizontal grid points. The GOTM then calculates one-dimensional profiles of TKE, dissipation rate, macroscopic length scale, and eddy viscosity and diffusivity. These are then composed back into three-dimensional fields.

For the shear production, a horizontal averaging of the vertical shear is needed due to the staggering of the grid. In a similar way, also the eddy viscosity has to be horizontally averaged before being used for the vertical turbulent transport in the momentum equations. In principle, such an averaging of the buoyancy-production term would not be necessary for the tracer equations, but experience shows that averaged weighting of some surrounding tracer values is needed for numerical stability.

26.5.3 Application to the Wadden Sea

Here, a numerical simulation of tidal currents in a Wadden Sea embayment, calculated with the latest version of the GETM, is presented. To do so, the tidal currents inside the so-called Sylt-Rømø Bight are simulated. This embayment is situated in the North Sea between the Danish island Rømø and the German island Sylt at about 55°N and 8°E and covers an area of about 300 km^2 ; see Fig. 26.8. The embayment is closed by marshlands to the east and artificial dams to the north and south. The tidal channel (Lister Tief) leading into the embayment has a width of about 2.5 km with a maximum depth of more than 30 m. Inside the bight, the Lister Tief branches into the Lister Ley to the south, the Hoyer Dyb to the southeast, and the Rømø Dyb to the northeast. The extensive tidal flat east of the Hoyer Dyb is called Jordsand; this was formerly a small island but has been eroded now. An interesting feature of the Sylt-Rømø Bight is the shallow embayment at the northern peak of Sylt, the so-called Königshafen.

The main forcing of the currents is the predominant M_2 tide with a tidal period of $T_4 = 44714\text{ s}$. There is no considerable inflow of freshwater into the embayment, so the water column is generally well mixed. Because of these ideal conditions (simple forcing, closed, well-mixed waters) the Sylt-Rømø Bight is a good test case for Wadden Sea models. Several authors have carried out simulations of this embayment (see e.g. Dick [1987], Burchard [1995], and Schneggenburger *et al.* [2000]).

For the present simulation, a bathymetry data set with a horizontal resolution of $200\text{ m} \times 200\text{ m}$ is used (see Fig. 26.8). An equidistant vertical discretization with $N = 20\sigma$ layers is chosen. A tidal forcing considering eight harmonic tides is applied until a periodically steady state is reached. For the momentum advection, a high-order total-variation-diminishing (TVD) scheme is used (Leonard, 1991; Leonard *et al.*, 1995). This one-dimensional scheme (also known as the ULTIMATE QUICKEST scheme) is here applied in a directional-split method with Strang (1968) splitting; see Pietrzak (1998). This third-order-in-space advection scheme guarantees low numerical diffusion and monotonicity of the advection operator.

The results for two different turbulence-closure models are presented here.

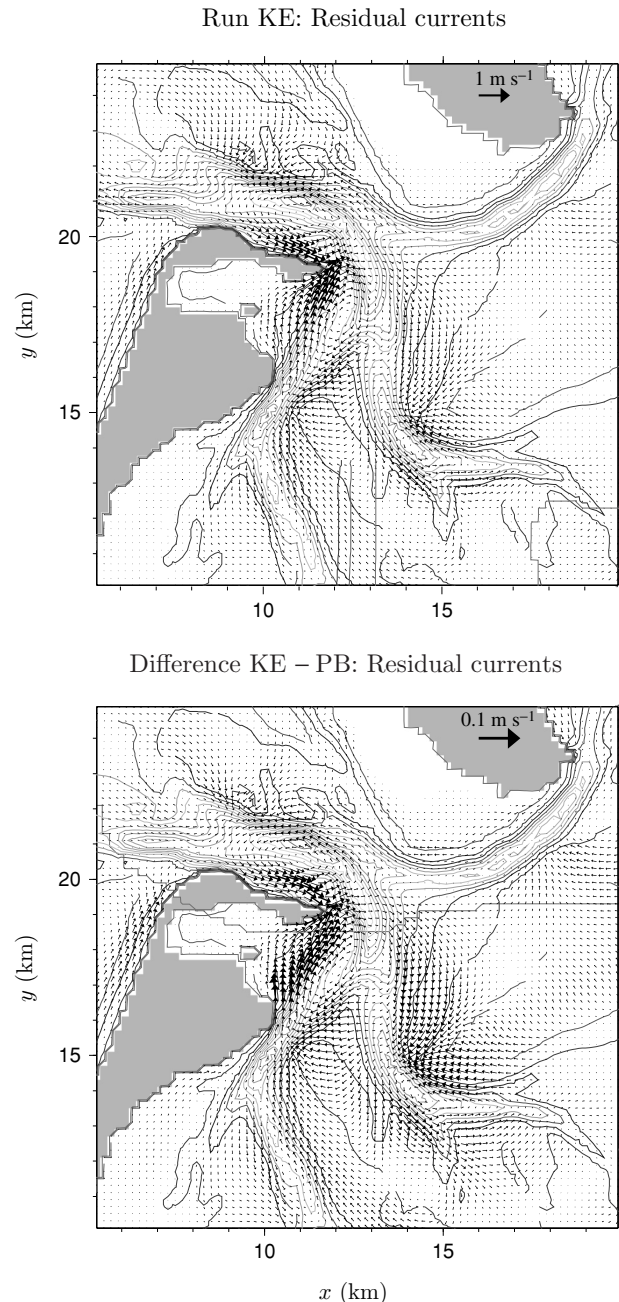


Fig. 26.9. Residual currents in the Sylt-Rømø Bight. Left: results for the $k-\varepsilon$ model; right: difference plot of results for the $k-\varepsilon$ model and results for a parabolic viscosity profile; see Eq. (26.3). In color on the CD.

KE As already used in Section 25.2 for one-dimensional water-column simulations, the two-equation $k-\varepsilon$ model combined with the algebraic second-moment closure recently suggested by Canuto *et al.* (2001) is applied here. In contrast to many other algebraic second-moment closures, which simply assume a

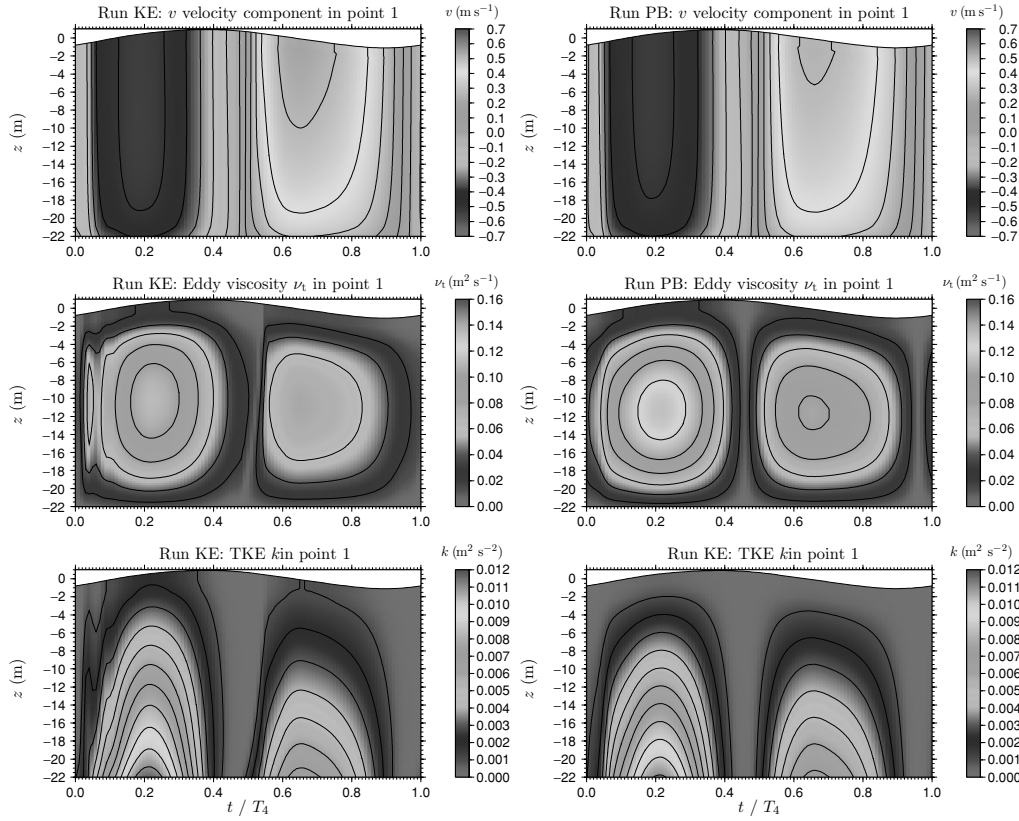


Fig. 26.10. The west–east velocity component u , eddy viscosity ν_t , and turbulence kinetic energy k during one tidal cycle at point 1. Left: results for run KE with a k - ε model; right: results for run PB with a parabolic eddy-viscosity profile. In color on the CD.

constant value for the stability functions (see e.g. Burchard and Bolding [2001]), this closure is a function of the current shear squared times the turbulence time scale squared. As surface and bottom boundary conditions, Neumann flux conditions for the TKE k and the dissipation rate are chosen; see Burchard and Petersen (1999).

PB In order to assess the performance of the complex turbulence closure model from run KE, the most basic assumptions for the TKE k and the macroscopic length scale L are made. The TKE k is assumed to decrease linearly from the surface upward, with a bottom value from the law of the wall:

$$k = \left(\frac{u_*^b}{c_\mu} \right)^2 \left(1 - \frac{z}{D} \right), \quad (26.1)$$

with the bottom friction velocity u_*^b , the constant stability function $c_\mu = 0.09$, the distance from the bed z , and the local water depth D . The macroscopic length scale L is assumed to have the shape of a distorted parabola see Xing and Davies (1995):

$$L = \kappa(z + z_0) \left(1 - \frac{z}{D} \right)^{1/2}, \quad (26.2)$$

with the bed roughness length z_0 and the von Kármán constant $\kappa = 0.4$. With (26.1) and (26.2), the following parabolic profile for the eddy viscosity can be derived:

$$\nu_t = \kappa u_*^b (z + z_0) \left(1 - \frac{z}{D} \right). \quad (26.3)$$

It can be shown that this profile results in a logarithmic velocity profile for steady-state flow; see Burchard *et al.* (1999).

Some results from the fifth tidal period after the initialization of the model are shown here. Figure 26.9 shows the tidal mean vertically averaged residual currents which can be calculated as follows:

$$u_r = \frac{\int_{T_4} U dt}{\int_{T_4} D dt}, \quad v_r = \frac{\int_{T_4} V dt}{\int_{T_4} D dt}. \quad (26.4)$$

with U and V being the instantaneous vertically integrated velocities in the x and y directions, respectively. General features are low residual currents in the deep channels and high residual currents at the shallow edges of these

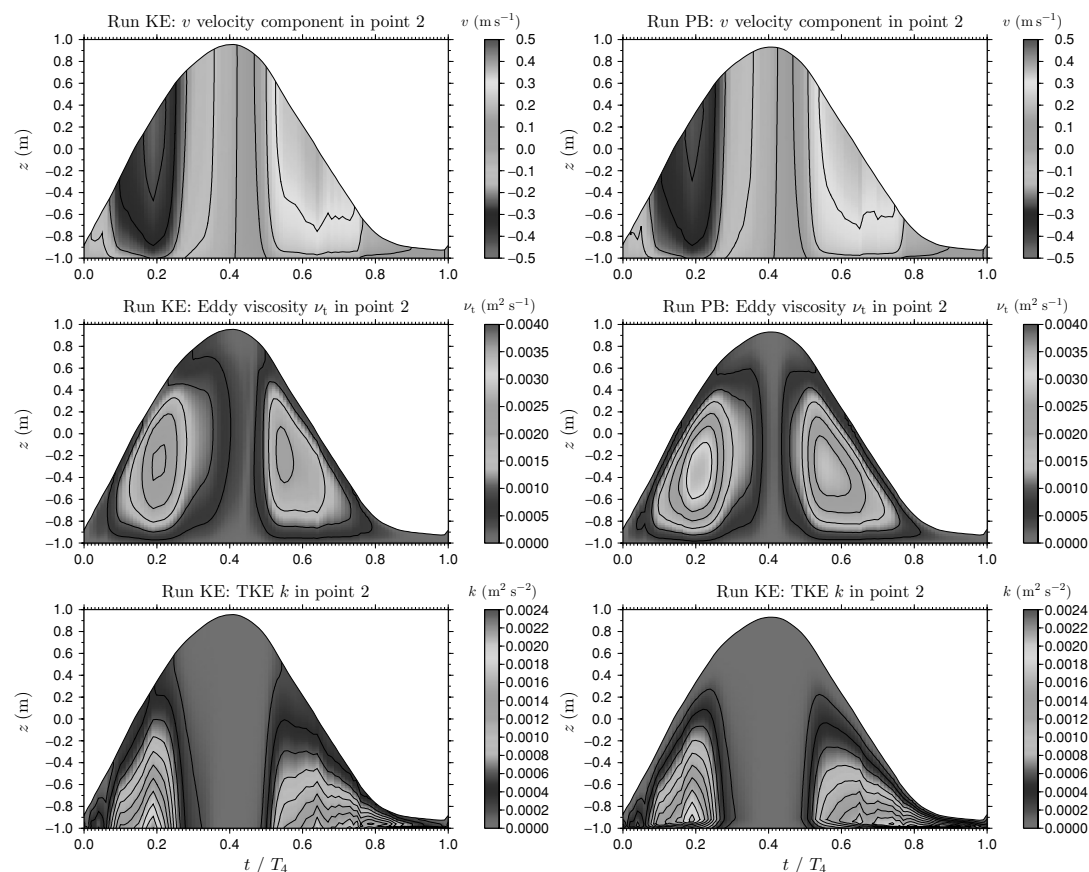


Fig. 26.11. The west–east velocity component u , eddy viscosity ν_t , and turbulence kinetic energy k during one tidal cycle at point 2. Left: results for run KE with a k – ϵ model; right: results for run PB with a parabolic eddy-viscosity profile. In color on the CD.

channels. Ebb dominance in the northern part of the Lister Tief and flood dominance in its southern part can clearly be seen. An inspection of the difference plot between runs KE and PB shows that the residual currents are generally smaller when the simple algebraic eddy-viscosity profile is used.

The reason for this is demonstrated in Figs. 26.10 and 26.11, where the temporal evolution of the water-column physics for a deep and for a shallow location is shown. At both locations, the eddy viscosities calculated by the simple model PB are considerably higher than those produced by the complex model KE. Therefore the vertical transport of momentum and the effect of bed friction are higher for the PB model. Owing to the algebraic nature of the PB model, turbulence profiles are instantaneously adjusted to the bed friction. In contrast to this, the turbulence calculated by the fully prognostic KE model is propagating upward with a significant time lag. One interesting feature can be observed at the deep location. The eddy viscosity and TKE exhibit a clear peak before the onset of the flood current ($t/T_4 = 0.05$). Such an enhancement of turbulence

after the flow reversal has already been shown to occur by Savioli and Justesen (1997) when simulating oscillatory sediment-laden flows with a k – ϵ model. This could have implications for simulating the dynamics of suspended matter; see e.g. the laboratory studies by Ribberink and Al-Salem (1992). This peak of vertical mixing is not present in the simple model PB, implying that simulation of suspended matter with this model would ignore some potentially important process.

It can be concluded from this Wadden Sea simulation that the use of high-order turbulence-closure models has an effect even on the transport in well-mixed regions, to which vertically integrated models are often applied for simplicity.

26.6 Summary and conclusions

The use of second-order turbulence closures provides a superior description of vertical mixing in a variety of oceanic regimes and is affordable in present-day three-dimensional simulations. With the aid of the GOTM, a one-dimensional model, the turbulence model has shown

its ability to represent vertical mixing in various situations (see Section 25.2)

We have shown in this chapter that the extensive testing of the turbulence module in a one-dimensional water-column model gives us confidence that new advances can be tested very rapidly in three-dimensional models and that a physically sound description of various mixing situations can be accomplished. Another interesting conclusion

of this work is that a modern approach to code development allows an easy and fast transfer of advances to other codes. Public-domain codes can rapidly achieve an up-to-date status. Apart from the model presented, we know of work in progress regarding coupling the GOTM to other widespread models such as the Princeton Ocean Model, Hamburg Ocean Primitive Equation Model, and Regional Ocean Model System.